RAPID COMMUNICATIONS

PHYSICAL REVIEW B VOLUME 38, NUMBER 8 15 SEPTEMBER 1988-I

Nonlinear dynamics of localization in a class of one-dimensional quasicrystals

Mark Holzer

Department of Physics, Simon Fraser University, Burnaby, British Columbia, V5A1S6, Canada

(Received 10 May 1988)

We consider the diagonalization of quasiperiodic operators on generalizations of the Fibonacci lattice defined recursively by $(A,B)\rightarrow(A^nB,A)$. The inflation symmetry of these lattices induces a three-dimensional nonlinear dynamical map on the traces of associated transfer matrices. We find the invariant manifolds for these trace maps to be twisted and pinched versions of the Fibonacci manifold. We investigate the effect of these pinches on the spectrum of a tight-binding Hamiltonian and consider the limit of weak incommensurability: $n\rightarrow\infty$.

In recent years much effort has been devoted to the study of quasicrystals in one dimension. Particularly well investigated is the Fibonacci lattice for which Kohmoto, Kadanoff, and Tang[1] developed the mathematical framework known as the KKT renormalization scheme. In this paper we extend the KKT scheme to the simplest class of recent generalizations of the Fibonacci lattice:[2] the precious mean (PM) lattices. (This nomenclature is consistent with the traditional assignment of the first few irrationals of this class to precious metals.) The PM lattices are labeled by an integer n and have the interesting property that their quasicrystallinity becomes arbitrarily weak, in the sense that their incommensurability approaches n, as $n\rightarrow\infty$. Previous work[2] showed that the inflation symmetry of the PM lattices induces, for all n, a three-dimensional (3D) nonlinear dynamical map on the traces of 2×2 unimodular transfer matrices defined on these lattices. Encouraged by the results of Gumbs and Ali,[3] we find the invariant manifold of these maps for all n, and identify their important cycles. Linearizing about these, we obtain the scaling indices for subsets of the zero Lebesgue measure multifractal spectrum of a simple diagonal tight-binding Hamiltonian. We then compare with numerical results and consider the limit $n\rightarrow\infty$.

The PM lattices are, like the Fibonacci lattice, two-tile Penrose tilings of the line and can be defined recursively by the inflation rule

$$(A,B)\rightarrow(A^nB,A)\,, \tag{1}$$

where A^n denotes a string of n A's. For $n=1$ this is the Fibonacci rule. The incommensurability of these lattices [the ratio of A's to B's in the infinite iterate of (1)] is $\tau_n=\frac{1}{2}(n+\sqrt{n^2+4})$. We call these irrationals the precious means. The number of A's in the kth iterate of (1) is F_k, the number of B's, F_{k-1}, where $F_k=nF_{k-1}+F_{k-2}$ are the PM numbers with $F_0=1$ and $F_1=n$. Explicitly, $F_k=[\tau^{k+1}+(-1)^k\tau^{-(k+1)}]/\sqrt{n^2+4}$.

Rather than considering physics in the world of the infinite PM lattice directly, it is natural to consider the same physics on a sequence of periodic lattices. The kth element of this sequence has the kth iteration of (1) as its unit cell and we call it the kth periodic approximation (PA). As $k\rightarrow\infty$ the sequence of PA's converges to the PM lattices. We restrict our discussion to problems reducible to the diagonalization of quasiperiodic operators whose eigenvalue equation can be cast in transfer matrix form with 2×2 transfer matrices of unit determinant. This includes a wide range of physical problems.[4,5] If M_k denotes the transfer matrix which takes us across a unit cell of the kth PA, then these transfer matrices obey, by virtue of inflation symmetry (1), the renormalization-group equation

$$M_{k+1}=M_{k-1}M_k^n\,. \tag{2}$$

As shown in Ref. 2, Eq. (2) implies a recursion relation for the traces of the transfer matrices which can be expressed as a 3D dynamical map. Defining $x\equiv\frac{1}{2}\mathrm{Tr}(M_{k-1})$, $y\equiv\frac{1}{2}\mathrm{Tr}(M_k)$, and $z_n\equiv\frac{1}{2}\mathrm{Tr}(M_{k+1})$,

$$\begin{pmatrix}x\\y\\z_n\end{pmatrix}\xrightarrow[T]{}\begin{pmatrix}y\\z_n\\z_n'(x,y,z_n)\end{pmatrix}, \tag{3}$$

where $z_n'(x,y,z)$ is given by Eq. (A13) of Ref. 2 as

$$z_n'\sum_{l_{\mathrm{odd}}=1}^{L}2(\mathrm{Tr}M_k^{n-l}-\delta_{n,l})+x\sum_{l_{\mathrm{odd}}=1}^{L}2(\mathrm{Tr}M_{k+1}^{n-l}-\delta_{n,l})$$
$$=\mathrm{Tr}M_{k+1}^n\,\mathrm{Tr}M_k^n+\sum_{r_{\mathrm{even}}=2}^{R}[\mathrm{Tr}M_{k+1}^n\,\mathrm{Tr}M_k^{n-r}+\mathrm{Tr}M_k^n\,\mathrm{Tr}M_{k+1}^{n-r}-\delta_{n,r}(\mathrm{Tr}M_{k+1}^n+\mathrm{Tr}M_k^n)]\,, \tag{4}$$

with $L\equiv n-[(n+1)\,\mathrm{mod}2]$ and $R\equiv n-(n\,\mathrm{mod}2)$. The traces of powers of matrices in (4) can be expressed as powers of traces of matrices as a simple consequence of the binomial theorem. Denoting the sum multiplying z_n' in (4) by $\eta_n(y)$, we discover, using the property of 2×2 unimodular matrices $\mathrm{Tr}[M_p^m(M_q^n+M_q^{-n})]=\mathrm{Tr}M_q^n\mathrm{Tr}M_p^m$, that

$$\eta_n(\xi)=2\xi\eta_{n-1}(\xi)-\eta_{n-2}(\xi)\,, \tag{5}$$

with $\eta_1(\xi)=2$ and $\eta_2(\xi)=4\xi$. We recognize (5) as the recursion relation for Chebyshev polynomials; in fact $\eta_n(\xi)=2U_{n-1}(\xi)$ where U_n is the nth Chebyshev polynomial of the second kind.[6] With this knowledge some algebra shows that (4) can be written succinctly as

$$z_n' = \frac{\eta_n(z)}{2\eta_n(y)}[z\eta_{n+1}(y)-2x]-\tfrac{1}{2}y\eta_{n-1}(z)\,. \tag{6}$$

To find the invariants of (3) for arbitrary n, consider the simplest possible nontrivial unimodular 2×2 matrices

$$M_0=\begin{bmatrix}2x & -1\\ 1 & 0\end{bmatrix} \text{ and } M_1=\begin{bmatrix}2y & -1\\ 1 & 0\end{bmatrix}. \tag{7}$$

With $2x=E-V_B$ and $2y=E-V_A$, these are the transfer matrices for the eigenvalue equation of the diagonal tight-binding Hamiltonian

$$H=\sum_j(\psi_{j+1}^{\dagger}\psi_j+\psi_j^{\dagger}\psi_{j+1}+V_j\psi_j^{\dagger}\psi_j)\,, \tag{8}$$

where $V_j=V_A$ or V_B depending on whether the jth site of the PM lattice is of type A or B. From (7) we obtain the third initial condition for the trace map

$$z_n=\tfrac{1}{2}\,\mathrm{Tr}(M_0M_1^n)=\tfrac{1}{2}\,[x\eta_{n+1}(y)-\eta_n(y)]\,. \tag{9}$$

The crucial step in finding the invariants of (3) is to realize that we can now map the flow of (3) onto the Fibonacci invariant manifold if we can make the transformation $z_n\rightarrow\tilde{z}_n=z_1$. Solving (9) for z_1, we see that this is indeed possible with

$$\tilde{z}_n=\frac{1}{\eta_n(y)}[x\eta_{n-1}(y)+2z_n]\,. \tag{10}$$

In terms of $\tilde{z}_n$, the invariant of (3) is then given by

$$I_n=x^2+y^2+\tilde{z}_n^2-2xy\tilde{z}_n-1\,, \tag{11}$$

which is independent of the choice (7) as can easily be proved by direct substitution of (3) into (11). We note that for model (8) $I_n=(x-y)^2=\frac{1}{4}(V_A-V_B)^2$ for all n.

We may consider $I_{n>1}(x,y,z_n)$ to have the same topology as I_1 (Refs. 7 and 8) in the sense that for $I_n<0$ the manifold consists of a central compact part and four infinite sheets (the compact part shrinks to a point at $I_n=-1$; for x,y,z real $I_n\geq -1$). When $I_n=0$ these sheets join the central part through four bottle necks which widen with increasing $I_n>0$. However, $I_{n>1}$ is a twisted version I_1 and may be visualized as follows: imagine twisting the two infinite sheets of I_1 in the half-space $y>0$ by $(n-1)\pi/2$ about the y axis. This twisting then results in pinching the central part of I_n off along line segments $z=(-1)^m x$, at the $n-1$ roots r_{nm} of $\eta_n(y)$ given by $r_{nm}=\cos(m\pi/n)$, $m\in\{1,2,\ldots,n-1\}$. The pinches extend from $-x_{\max}$ to $x_{\max}$, where $x_{\max}=[(a^2-r_{nm}^2)/(1-r_{nm}^2)]^{1/2}$ and $a^2\equiv I_n+1$.

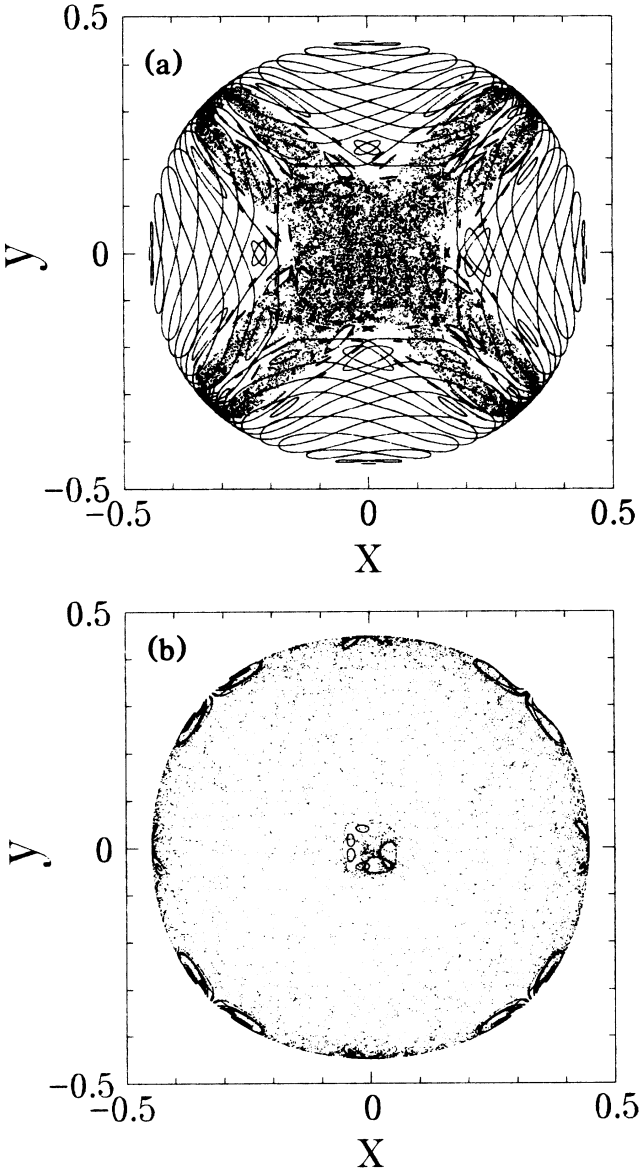

FIG. 1. Flow of the PM trace map on the compact part of $I_n=-0.8$ projected onto the xy plane. (a) $n=2$: 18 selected seeds have been iterated 10000 times. The flow about the four-cycle (figure eights) and zero-root-cycle (stochastic bands) is apparent. The four-cycle at $(0,\pm\sqrt{0.2},0)$ is elliptic. (b) $n=5$: 23 seeds have been iterated 2500 times. Elliptic satellites of the six-cycle and $r_{5,2}$ and $r_{5,3}$ root cycles are clearly visible.

For $I_n>0$ all the cycles of the PM trace map (3) appear to be unstable. For $I_n<0$, some cycles are elliptic, but become hyperbolic via bifurcation before I_n reaches zero. The cycles dominating the flow of (3) close to $I_n=-1$ on the compact part of I_n are (see Fig. 1), for n odd, the six-cycles

$$\begin{bmatrix}x\\y\\z\end{bmatrix}=\begin{bmatrix}0\\0\\a\end{bmatrix}\rightarrow\begin{bmatrix}0\\a\\0\end{bmatrix}\rightarrow\begin{bmatrix}a\\0\\0\end{bmatrix}\rightarrow\begin{bmatrix}0\\0\\-a\end{bmatrix}\rightarrow\begin{bmatrix}0\\-a\\0\end{bmatrix}\rightarrow\begin{bmatrix}-a\\0\\0\end{bmatrix}\rightarrow\begin{bmatrix}0\\0\\a\end{bmatrix}, \tag{12}$$

and, for n even the four-cycles (two-cycles if $n/2$ is even)

$$\begin{bmatrix} x \\ y \\ z \end{bmatrix} = \begin{bmatrix} 0 \\ a \\ 0 \end{bmatrix} \rightarrow \begin{bmatrix} a \\ 0 \\ (-1)^{n/2}a \end{bmatrix} \rightarrow \begin{bmatrix} 0 \\ (-1)^{n/2}a \\ 0 \end{bmatrix} \rightarrow \begin{bmatrix} (-1)^{n/2}a \\ 0 \\ a \end{bmatrix} \rightarrow \begin{bmatrix} 0 \\ a \\ 0 \end{bmatrix}. \tag{13}$$

The six-cycle lies entirely on analytic patches of I_{odd} and we calculate the eigenvalues of T^6 linearized about (12) to be

$$\lambda_6 = \frac{\omega_6}{2} \pm \left[\left(\frac{\omega_6}{2} \right)^2 - 1 \right]^{1/2}, \tag{14}$$

with

$$\omega_6 = \frac{\zeta^4}{4\eta_n^2} + \zeta^2 \left(\frac{1}{2} - \frac{2}{\eta_n^2} \right) + \frac{4}{\eta_n^2} + \frac{\eta_n^2}{4} \tag{15}$$

where $\zeta \equiv a(n-1)\eta_n + \eta_{n+1}$, and the argument of the Chebyshev polynomials is a. The nonanalyticity of I_n on its pinches causes trace map orbits to cross there (as they flow on interpenetrating sheets of I_n) and gives rise to a class of cycles, which we call root cycles, lying entirely on the pinches (see Fig. 1). While the four-cycle (13) is not a root-cycle, it lies partly on the $y=0$ pinch of I_{even} and linearization about it must, as in the case of the root cycles, deal with the technical subtleties arising from the nonanalyticity of the pinches. This difficulty is most easily handled by mapping (3) onto the analytic Fibonacci manifold using transformation (10). The thus transformed map may be written

$$\begin{bmatrix} x \\ y \\ \tilde{z} \end{bmatrix} \xrightarrow{\tilde{T}} \begin{bmatrix} y \\ \frac{1}{2}[\tilde{z}\eta_n(y) - x\eta_{n-1}(y)] \\ \frac{1}{2}[\tilde{z}\eta_{n+1}(y) - x\eta_n(y)] \end{bmatrix}. \tag{16}$$

Because x and y remain unchanged, this map has the advantage of being analytic while preserving the cycles and linear eigenvalues of (3). Writing the four-cycles (13) in terms of (16) and linearizing, we find

$$\lambda_4 = \frac{\omega_4}{2} \pm \left[\left(\frac{\omega_4}{2} \right)^2 - 1 \right]^{1/2} \tag{17}$$

with

$$\omega_4 = \tfrac{1}{4}[2\eta_{n-1}(a) - a(n+2)\eta_n(a)]^2 - 2. \tag{18}$$

The general two-cycle of (3), $x \rightarrow y \rightarrow x$, is determined by the condition $2 - g(y) = g(x)$, with $g(\xi) \equiv [\eta_{n-1}(\xi)+2]/[\xi\eta_n(\xi)]$.

The root cycles for n odd are

$$\begin{bmatrix} x \\ y \\ \tilde{z} \end{bmatrix} = \begin{bmatrix} r_{nm} \\ \pm r_{nm} \\ \pm b \end{bmatrix} \rightarrow \begin{bmatrix} \pm r_{nm} \\ \pm(-1)^m r_{nm} \\ (-1)^m b \end{bmatrix} \rightarrow \begin{bmatrix} \pm(-1)^m r_{nm} \\ r_{nm} \\ \pm(-1)^m b \end{bmatrix} \rightarrow \begin{bmatrix} r_{nm} \\ \pm r_{nm} \\ \pm b \end{bmatrix}. \tag{19}$$

and the root cycles for n even are

$$\begin{bmatrix} x \\ y \\ \tilde{z} \end{bmatrix} = \begin{bmatrix} r_{nm} \\ \pm r_{nm} \\ \pm b \end{bmatrix} \rightarrow \begin{bmatrix} \pm r_{nm} \\ (-1)^m r_{nm} \\ \pm(-1)^m b \end{bmatrix} \rightarrow \begin{bmatrix} (-1)^m r_{nm} \\ \pm(-1)^m r_{nm} \\ \pm b \end{bmatrix} \rightarrow \begin{bmatrix} \pm(-1)^m r_{nm} \\ r_{nm} \\ \pm(-1)^m b \end{bmatrix} \rightarrow \begin{bmatrix} r_{nm} \\ \pm r_{nm} \\ \pm b \end{bmatrix}, \tag{20}$$

where $b = r_{nm}^2 \pm (r_{nm}^4 - 2r_{nm}^2 + a^2)^{1/2}$. The effect of $\tilde{T}$ on a point of a root cycle is to merely change the signs of its coordinates. Furthermore, we find that the maximum eigenvalues of the cycles (19) and (20) are powers of λ_1 given below. We may therefore regard the root cycles as effective one-cycles, or fixed points, which are, for sufficiently large I_n, hyperbolic with the eigenvalue of the unstable manifold given by

$$|\lambda_1| = \frac{\omega_1}{2} + \left[\left(\frac{\omega_1}{2} \right)^2 + 1 \right]^{1/2}, \tag{21}$$

where

$$\omega_1 = n \frac{(r_{nm}^4 - 2r_{nm}^2 + a^2)^{1/2}}{1 - r_{nm}^2}. \tag{22}$$

Consider now, for definiteness, the diagonalization of Hamiltonian (8). In the kth PA, its spectrum is determined by the condition $|x_k(E)| \leq 1$, where $x_k(E) \equiv \frac{1}{2}\,\text{Tr}M_k(E)$ with M_0 and M_1 given by (7). $x_k(E)$ is a polynomial of order F_k whose roots are bounded by $(E_{\min}, E_{\max}) = (\min(V_A, V_B) - 2, \max(V_A, V_B) + 2)$ and whose local extrema exceed 1 in absolute value. As $k \rightarrow \infty$, $x_k(E)$ traverses the strip $|x_k(E)| \leq 1$ increasingly fast and the spectrum of (8), consisting of F_k bands forming a hierarchy of band clusters, converges to a zero Lebesgue measure multifractal.[1,2] As a consequence of Eq. (2) the corresponding states are critical, that is, power-law localized.[8]

A multifractal can be characterized by a spectrum of fractal dimensions $f(\alpha)$ which has the general properties $\alpha \in [\alpha_{\min}, \alpha_{\max}]$, $\partial^2 f/\partial\alpha^2 < 0$, $\partial f/\partial\alpha|_{f=\alpha} = 1$, and $\max[f(\alpha)] = D_H$, the Hausdorff dimension of the multifractal.[9] For model (8), α is the scaling index for the set of bands whose bandwidths ΔE scale with their integrated density of states $1/F_k$ like ΔE^{α}. Writing $x_k(E)$

$\approx 2(E-E_j)/\Delta E_j$, where $\Delta E_j = 2/(\partial x/\partial E)\,|_{Ej}$ and E_j is a root of $x_k(E)$ resulting in a band of width ΔE_j, we see that the width of a band at energy E goes to zero at the same rate as $x_k(E)$ escapes to infinity. Thus, the scaling index for the set of bands which puts $x_k(E)$ in the vicinity of a hyperbolic Q-cycle, where $x_k(E)$ grows exponentially with k like $\lambda_Q^{k/Q}$, is given by $\alpha_Q = Q\log\tau_n/\log\lambda_Q$. (A formalism for calculating localization exponents of the corresponding states may be found in Ref. 10.)

Numerically we find that the centers of the band clusters of the spectrum of (8), for n odd, scale like the six-cycles (12). However for $n > 1$ the spectrum is no longer fattest there, that is, the centers no longer scale with $\alpha_{\max}$ as in the Fibonacci case; in fact

$$\alpha_6 \rightarrow \frac{3\log n}{n\log[(a^2-1)^{1/2}+a]} \quad \text{as } n\rightarrow\infty\,, \tag{23}$$

which goes to zero. The four-cycles (13) do *not* govern the scaling of the cluster centers which *are* the fattest part of the spectrum for n even. Like α_6, α_4 asymptotically goes to zero:

$$\alpha_4 \rightarrow \frac{2\log n}{n\log[(a^2-1)^{1/2}+a]} \quad \text{as } n\rightarrow\infty\,. \tag{24}$$

We note that this is contrary to the claims of Gumbs and Ali.[3]

Let the scaling index for sets governed by the root cycle of root r_{nm} be denoted by α_{nm}. From (21) and (22) we note that α_{nm} is largest for the smallest roots. $\alpha_{\max}$, obtained numerically using the algorithm of Ref. 9, and $\alpha_{n,n/2}$, for n even, are in excellent agreement. For n odd, $\alpha_{n,(n\pm1)/2}$ appear to agree well with $\alpha_{\max}$ for $n > 3$. For example, for $n = 2,3,4,5, (\alpha_{\max}, \alpha_{nm})$ of the spectrum of (8), with $I_n = \frac{1}{4}$, are calculated to be (0.916, 0.9158), (0.90, 0.8838), (0.935, 0.9347), and (0.93, 0.9295), respectively. (For $n = 1,2,3,4,5$, the numerically obtained D_H are 0.7729, 0.7745, 0.7766, 0.7811, and 0.7857.) Discrepancies for n odd may either be due to another cycle governing the fattest parts of the spectrum or to the nonuniform convergence of the numerical result observed for n odd.[2] For fixed $m/n \equiv \rho$, α_{nm} converges to 1 like

$$\alpha_{n,\rho n} \rightarrow 1\Big/\left(1+\frac{\log(\omega_1/n)}{\log n}\right) \quad \text{as } n\rightarrow\infty\,. \tag{25}$$

For m fixed, α_{nm} converges to $\frac{1}{3}$ like

$$\alpha_{nm} \rightarrow 1\Big/\left(3+\frac{\log[\sqrt{I}/(m^2\pi^2)]}{\log n}\right) \quad \text{as } n\rightarrow\infty\,. \tag{26}$$

If $\Omega_r(\alpha_{nm})d\alpha$ denotes the number of $\alpha_{nm} \in (\alpha, \alpha+d\alpha)$, Eqs. (22) and (25) show that $\Omega_r(\alpha_{nm})$ is sharply peaked close to 1 and approaches $n\delta(\alpha-1)$ as $n\rightarrow\infty$. The trend observed numerically[2] for $f(\alpha)$ together with Eqs. (23)–(25), the convexity of $f(\alpha)$, the boundedness of $f(\alpha)$ by α from above, and the asymptotic behavior of $\Omega_r(\alpha_{nm})$ strongly suggest that $f(\alpha)\rightarrow\alpha$, with $\alpha \in (0,1)$, as $\tau_n \rightarrow n$. As we can see from (25), convergence to this limit is extremely slow. We conjecture that $f = \alpha$ may also be the form of the $f(\alpha)$ curve at criticality for quasicrystalline systems which undergo a phase transition. Evidence for this is suggested in the critical $f(\alpha)$ curve of Ref. 11.

During the course of this work I have benefited from discussions with K. Heiderich, M. Plischke, and M. Wortis.

[1] M. Kohmoto, L. P. Kadanoff, and C. Tang, Phys. Rev. Lett. **50**, 1870 (1983).

[2] Mark Holzer, Phys. Rev. B **38**, 1709 (1988).

[3] Godfrey Gumbs and M. K. Ali, Phys. Rev. Lett. **60**, 1081 (1988).

[4] A. H. MacDonald and G. C. Aers, Phys. Rev. B **36**, 9142 (1987).

[5] Bill Sutherland, Phys. Rev. Lett. **57**, 770 (1986).

[6] I. S. Gradshteyn and I. M. Ryzhik, *Tables of Integrals, Series, and Products* (Academic, New York, 1980), p. 1032.

[7] M. Kohmoto and Y. Oono, Phys. Rev. Lett. **102A**, 145 (1984).

[8] Mahito Kohmoto, Bill Sutherland, and Chao Tang, Phys. Rev. B **35**, 1020 (1987).

[9] Thomas C. Halsey, Morgens H. Jensen, Leo P. Kadanoff, Itamar Procaccia, and Boris I. Shraiman, Phys. Rev. A **33**, 1141 (1986).

[10] Bill Sutherland, Phys. Rev. B **35**, 9529 (1987).

[11] Mauro M. Doria and Indubala I. Satija, Phys. Rev. Lett. **60**, 444 (1988).

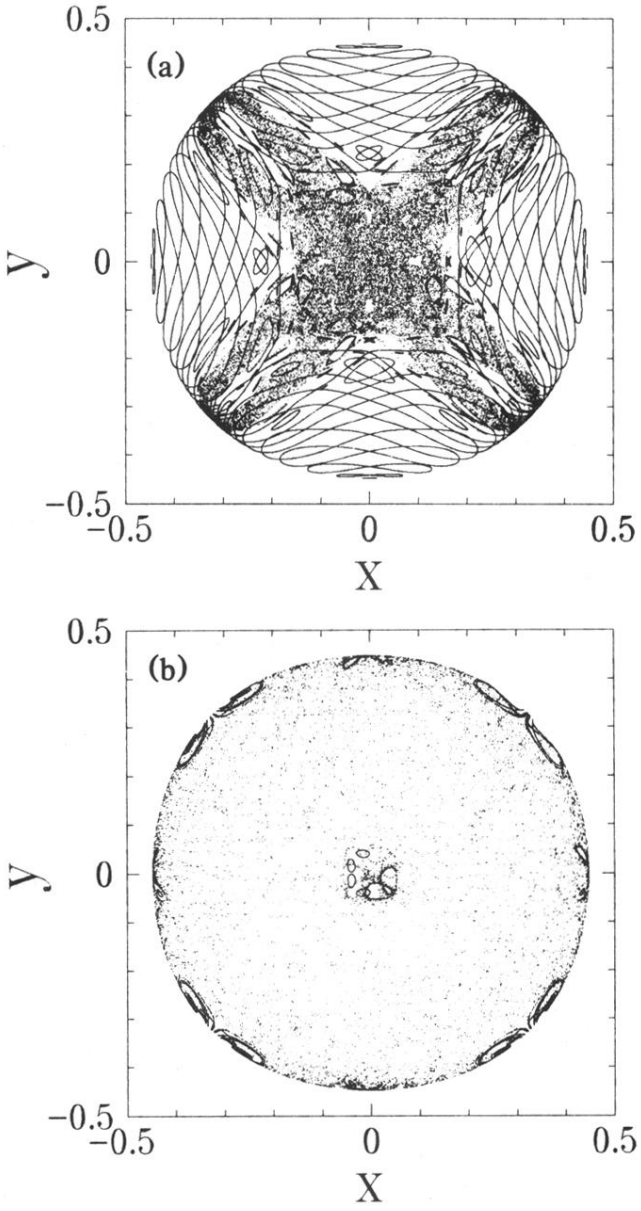

FIG. 1. Flow of the PM trace map on the compact part of $I_n = -0.8$ projected onto the xy plane. (a) $n=2$: 18 selected seeds have been iterated 10000 times. The flow about the four-cycle (figure eights) and zero-root-cycle (stochastic bands) is apparent. The four-cycle at $(0, \pm\sqrt{0.2}, 0)$ is elliptic. (b) $n=5$: 23 seeds have been iterated 2500 times. Elliptic satellites of the six-cycle and $r_{5,2}$ and $r_{5,3}$ root cycles are clearly visible.